



## OPEN

Production of salidroside in metabolically engineered *Escherichia coli*

## SUBJECT AREAS:

BIOTECHNOLOGY  
METABOLIC ENGINEERINGYanfeng Bai<sup>1,2,3\*</sup>, Huiping Bi<sup>1,2\*</sup>, Yibin Zhuang<sup>1,2</sup>, Chang Liu<sup>1,2,3</sup>, Tao Cai<sup>1</sup>, Xiaonan Liu<sup>1,2,3</sup>, Xueli Zhang<sup>1,2</sup>, Tao Liu<sup>1,2</sup> & Yanhe Ma<sup>1</sup>Received  
14 July 2014Accepted  
29 September 2014Published  
17 October 2014Correspondence and  
requests for materials  
should be addressed to  
T.L. (liu\_t@tib.cas.cn)\* These authors  
contributed equally to  
this work.

<sup>1</sup>Tianjin Institute of Industrial Biotechnology, Chinese Academy of Sciences, Tianjin 300308, China, <sup>2</sup>Key Laboratory of Systems Microbial Biotechnology, Chinese Academy of Sciences, Tianjin 300308, China, <sup>3</sup>University of Chinese Academy of Sciences, Beijing, China.

Salidroside (1) is the most important bioactive component of *Rhodiola* (also called as “Tibetan Ginseng”), which is a valuable medicinal herb exhibiting several adaptogenic properties. Due to the inefficiency of plant extraction and chemical synthesis, the supply of salidroside (1) is currently limited. Herein, we achieved unprecedented biosynthesis of salidroside (1) from glucose in a microorganism. First, the pyruvate decarboxylase ARO10 and endogenous alcohol dehydrogenases were recruited to convert 4-hydroxyphenylpyruvate (2), an intermediate of L-tyrosine pathway, to tyrosol (3) in *Escherichia coli*. Subsequently, tyrosol production was improved by overexpressing the pathway genes, and by eliminating competing pathways and feedback inhibition. Finally, by introducing *Rhodiola*-derived glycosyltransferase UGT73B6 into the above-mentioned recombinant strain, salidroside (1) was produced with a titer of 56.9 mg/L. Interestingly, the *Rhodiola*-derived glycosyltransferase, UGT73B6, also catalyzed the attachment of glucose to the phenol position of tyrosol (3) to form icariside D2 (4), which was not reported in any previous literatures.

Salidroside (1), a glucoside of tyrosol (3)<sup>1,2</sup>, was well established as the main bioactive component of *Rhodiola*<sup>3,4</sup> (also known as “Tibetan Ginseng”), which is a highly valued medicinal herb that grows at high altitude and in cold regions, such as the slopes of the Himalayas. Its benefits date back to a long history of folk use. It is known to play an important role in adaptogenic effects, like treating anoxia, microwave radiation, fatigue, and slowing the aging process<sup>5,6</sup>. Reports have shown that it can also prevent cardiovascular diseases and cancer<sup>7,8</sup>. No side effects or drug interactions have been reported for *Rhodiola*<sup>9</sup>. The aglycon tyrosol (3) is also present in *Rhodiola* and displays multiple pharmacological effects. As a natural phenolic antioxidant, tyrosol (3) can protect cells against injury due to oxidation. In addition, it has been shown to play a role in the prevention of cardiovascular diseases<sup>10,11</sup>, osteopenia<sup>12</sup>, melanin pigmentation<sup>13</sup>, as well as in anti-inflammatory responses<sup>14</sup>.

Because of its slow growth and over-gathering, the resources of wild *Rhodiola* are on the edge of exhaustion<sup>2</sup>. Furthermore, the content of salidroside (1) in *Rhodiola* is relatively low<sup>1</sup>. Hence, to meet the increasing demands, considerable efforts have been made on enhancing the production of salidroside (1) since many years; and these include extensive field cultivation, tissue culture, and genetic engineering of *Rhodiola*<sup>2,15–17</sup>. However, these processes are expensive, time-consuming, and produce low yields, and as a result, cannot be used extensively. It is, therefore, urgent to establish alternative ways to produce salidroside (1).

Researchers have engineered genetically tractable microorganisms to carry out secondary metabolic pathways in plants, in order to produce a range of natural products<sup>18–21</sup>. Development of an effective protocol and strain for the microbial production of salidroside (1) using renewable feedstock might be a commercially valuable process. *Escherichia coli* (*E. coli*) has emerged as a “user-friendly” heterologous host due to its rapid growth rate, simple culture conditions, plethora of readily accessible genetic tools, and comprehensive synthetic biological framework<sup>22–25</sup>.

While the biosynthetic pathway of salidroside (1) is still elusive<sup>15</sup>, two pathways for the formation of tyrosol (3) are established in nature. The first pathway involves the conversion of L-tyrosine into tyramine by tyrosine decarboxylase (TDC); and further transformation of tyramine into tyrosol by tyramine oxidase (TYO) and alcohol dehydrogenase (ADH), consecutively<sup>26</sup>. Besides, tyrosol (3) can also be derived from yeast Ehrlich pathway, by conversion of L-tyrosine through the sequential action of aminotransferase, pyruvate decarboxylase, and ADHs (Fig. 1a)<sup>27,28</sup>. In a study by Yu *et al.*, the glycosyltransferase UGT73B6 was isolated from *Rhodiola sachalinensis*, and the enzyme was found to be able to convert tyrosol into salidroside<sup>29</sup>.

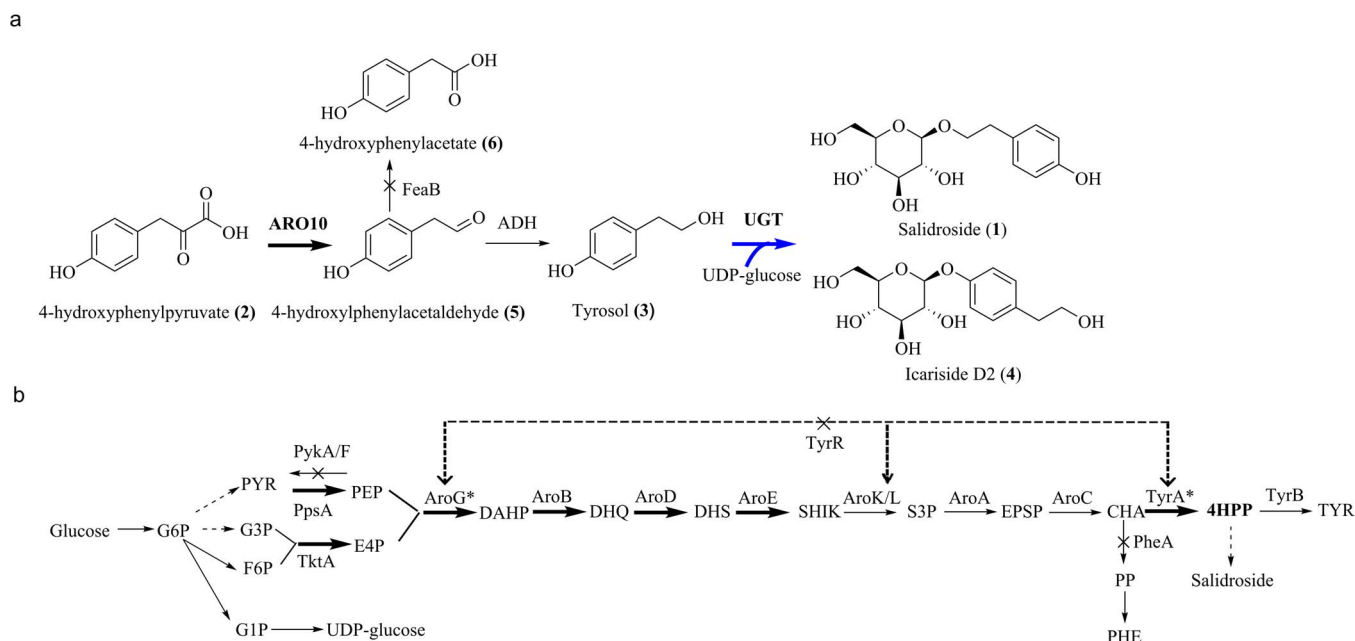


**Figure 1 | Metabolic pathways for tyrosol (3), salidroside (1), and icaricide D2 (4) biosynthesis in recombinant *E. coli* strains from glucose.** (a) The artificial synthetic pathway for salidroside (1) production from 2 consisting of enzymes, yeast pyruvate decarboxylase ARO10, endogenous ADH of *E. coli*, and UGT73B6 from *Rhodiola*. (b) Metabolic flux enhancement of precursor supply of 2. Single arrows represent one-step conversions, while single dashed arrows represent multiple steps. Bold arrows represent gene overexpression. The dashed lines indicate feedback inhibitions. The fork arrows represent gene deletion. Abbreviations: G6P, 6-phosphate-D-glucose; PYR, pyruvate; G3P, glyceraldehyde-3-phosphate; F6P, fructose-6-phosphate; PEP, phosphoenolpyruvate; E4P, erythrose 4-phosphate; UDP-glucose, Uridine 5'-diphosphoglucose; DAHP, 3-deoxy-arabino-heptulonate7-phosphate; DHQ, 3-dehydroquinic acid; CHA, chorismic acid; DHS, dehydroshikimate; SHIK, shikimate; S3P, shikimate 3-phosphate; EPSP, 5-enolpyruvylshikimate-3-phosphate; CHA, chorismate; PP, phenylpyruvate; PHE, phenylalanine; 4HPP, 4-hydroxyphenylpyruvate; TYR, tyrosine; AroG\*, feedback resistant mutant of AroG; TyrA\*, feedback resistant mutant of TyrA; FeaB, phenylacetaldehyde dehydrogenase; ADH, alcohol dehydrogenase.

In the present study, we first engineered *E. coli* to synthesize tyrosol (3) from glucose by the integration of a yeast pyruvate decarboxylase ARO10 into the L-tyrosine pathway (Fig. 1). Subsequently, we improved production of tyrosol (3) through enhancement of metabolic flux towards 4-hydroxyphenylpyruvate (2) by the metabolic engineering of L-tyrosine pathways into *E. coli* (Fig. 1b). Finally, we introduced plant-derived UGT73B6 into this recombinant *E. coli* strain and accomplished the unprecedented biosynthesis of salidroside (1) in a microbial system. Moreover, the *Rhodiola*-derived glycosyltransferase UGT73B6 catalyzed the formation of icaricide D2 (4) by adding glucose to the phenolic position of tyrosol (3), which was reported for the first time regarding the function of the glycosyltransferase.

## Results

**Construction of the tyrosol biosynthetic pathway in *E. coli*.** First, we attempted to construct a metabolic pathway for the production of tyrosol (3) in *E. coli*. In the yeast Ehrlich pathway, the key intermediate, 4-hydroxyphenylpyruvate (2), is derived from L-tyrosine by transamination; while in *E. coli*, this compound is a native metabolite in the L-tyrosine biosynthetic pathway. Compound 2 was decarboxylated to 4-hydroxyphenylacetaldehyde (5) by the expression of a pyruvate decarboxylase gene ARO10 from *Saccharomyces cerevisiae*<sup>27</sup>. Compound 5 was reduced to tyrosol by the endogenous ADHs in *E. coli* (Fig. 1a). Besides reduction to tyrosol, the intermediate compound 5 could also be oxidized to 4-hydroxyphenylacetate (6) by the endogenous phenylacetaldehyde dehydrogenase (FeaB or PadA) of *E. coli*<sup>26</sup>. To enhance the production of tyrosol, we constructed a *feaB*-knockout strain (BMGF0, Table 1), thus shutting off the synthesis pathway of compound 6.

As shown in Fig. 2, the *feaB*-knockout strain harboring the ARO10 gene (BMGF1) was able to produce a new compound corresponding to peak I (Fig. 3a) in the HPLC chromatogram with identical retention time as tyrosol (3). The structure was further confirmed by a positive high-resolution electrospray mass spectrometry (HR-ESI-MS) at  $m/z$  121.0680  $[M-H_2O + H]^+$  (Fig. 3b). The experiment demonstrated that tyrosol (3) production from glucose was enabled in *E. coli* by the introduction of phenylpyruvate decarboxylase ARO10 from yeast. Fermentation led to the production of 128.3 mg/L of tyrosol (3) from 2% glucose in flask cultures.

**Enhancement of tyrosol production by elimination of competitive pathways and negative regulation.** To improve the capacity of the strain for tyrosol (3) production from glucose, we further enhanced metabolic flux towards 4-hydroxyphenylpyruvate (2) in *E. coli*. The negative regulatory and competing pathways were eliminated in the biosynthesis of L-tyrosine (Fig. 1b). In concrete terms, the pathway-specific transcriptional regulatory gene, *tyrR*, was inactivated, which in turn led to the enhanced expression of genes relevant to L-tyrosine biosynthesis, including *aroG*, *tyrA*, and *aroL*, encoding 3-deoxy-D-arabino-heptulosonate (DAHP) synthase, chorismate mutase/prephenate dehydrogenase, and shikimate kinase, respectively<sup>30,31</sup>. Both *pykA* and *pykF* genes encoding the pyruvate kinase isozymes were knocked out to block the metabolic flux associated with the conversion of phosphoenolpyruvate (PEP) to pyruvate, further intensifying the availability of PEP to synthesize more DAHP. In addition, the *pheA* gene was deleted to prevent the competitive L-phenylalanine biosynthesis, thereby driving chorismate to the production of 4-hydroxyphenylpyruvate (2) and L-tyrosine (Fig. 1b). Following these manipulations in the genome of the tyrosol-producing *E. coli* strain BMGF1, the yield of tyrosol (3) was found to increase gradually from 128.3 mg/L to 603.9 mg/L



Table 1 | Bacterial strains and plasmids

Name	Description	Reference
<b>Strains</b>		
BMGF	<i>E. coli</i> MG1655 $\Delta feaB$	This study
BMGF0	<i>E. coli</i> MG1655 $\Delta feaB$ with pTrcHisB	This study
BMGF1	<i>E. coli</i> MG1655 $\Delta feaB$ with pTrc1	This study
BMGP	BMGF $\Delta pykA$	This study
BMGP1	BMGP with pTrc1	This study
BMGT	BMGP $\Delta tyrR$	This study
BMGT1	BMGT with pTrc1	This study
BMGK	BMGT $\Delta pykF$	This study
BMGK1	BMGK with pTrc1	This study
BMGA	BMGK $\Delta pheA$	This study
BMGA1	BMGA with pTrc1	This study
BMGA2	BMGA with pTrc1 & pBb0	This study
BMGA3	BMGA with pTrc1 & pBb1	This study
BMGA4	BMGA with pTrc1 & pBb2	This study
BMGA5	BMGA with pTrc1 & pBb3	This study
BMGA6	BMGA with pTrc2 & pBb3	This study
<b>Plasmids</b>		
pKD46	Red recombinase expression vector; Amp <sup>R</sup>	(Datsenko and Wanner, 2000)
pKD4	FRT (FLP recognition target) sites; Kan <sup>R</sup>	(Datsenko and Wanner, 2000)
pCP20	FLP expression vector; Amp <sup>R</sup>	(Datsenko and Wanner, 2000)
pTrcHisB	pTrcHisB, pBR322 ori with P <sub>Trc</sub> ; Amp <sup>R</sup>	Invitrogen
pTrc1	pTrcHisB with P <sub>Trc</sub> -ARO10; Amp <sup>R</sup>	This study
pTrc2	pTrcHisB with P <sub>Trc</sub> -ARO10-P <sub>Trc</sub> -UGT73B6; Amp <sup>R</sup>	This study
pACYCDuet-1	P15A ori with P <sub>T7</sub> ; Cm <sup>R</sup>	Novagen
pBba5c	p15A ori, Cm <sup>R</sup>	(Lee, et al., 2011)
pBb0	pBba5c with a new MCS, p15A ori, Cm <sup>R</sup>	This study
pBb1	pBba5c-MCS with P <sub>Ltet</sub> -tyrA*-aroG*-ppsA, Cm <sup>R</sup>	This study
pBb2	pBba5c-MCS with P <sub>Ltet</sub> -tyrA*-aroG*-ppsA and P <sub>lacUV5</sub> -tktA-aroE, Cm <sup>R</sup>	This study
pBb3	pBba5c-MCS with P <sub>Ltet</sub> -tyrA*-aroG*-ppsA, P <sub>lacUV5</sub> -tktA-aroE and P <sub>lacUV5</sub> -aroD-aroB <sup>op</sup> , Cm <sup>R</sup>	This study

using 2% glucose under the 50 mL shake-flask cultivation (Fig. 3c). Among the four targeted genes, the deletion of *pheA* contributed considerably to the increment of tyrosol (3) yield, from 347.3 mg/L to 603.9 mg/L (Fig. 3c).

**Enhancement of tyrosol production by overexpression of pathway genes.** In order to further enhance the metabolic flux towards 4-hydroxyphenylpyruvate (2), several key genes in the pathway were

expressed (Fig. 1b and 2). Firstly, the feedback-resistant mutants, *aroG*\*<sup>syn</sup> (D146N) and *tyrA*\*<sup>syn</sup> (M53I; A354V) were expressed under the control of a constitutive P<sub>LtetO-1</sub> promoter. The *aroG* encoding DAHP synthase and *tyrA* encoding chorismate mutase/prephenate dehydrogenase, catalyzed formations of DAHP or 4-hydroxyphenylpyruvate (2) respectively, in the biosynthesis of L-tyrosine. These two committed steps were tightly regulated by aromatic amino acids. The feedback-resistant derivatives, AroG\*

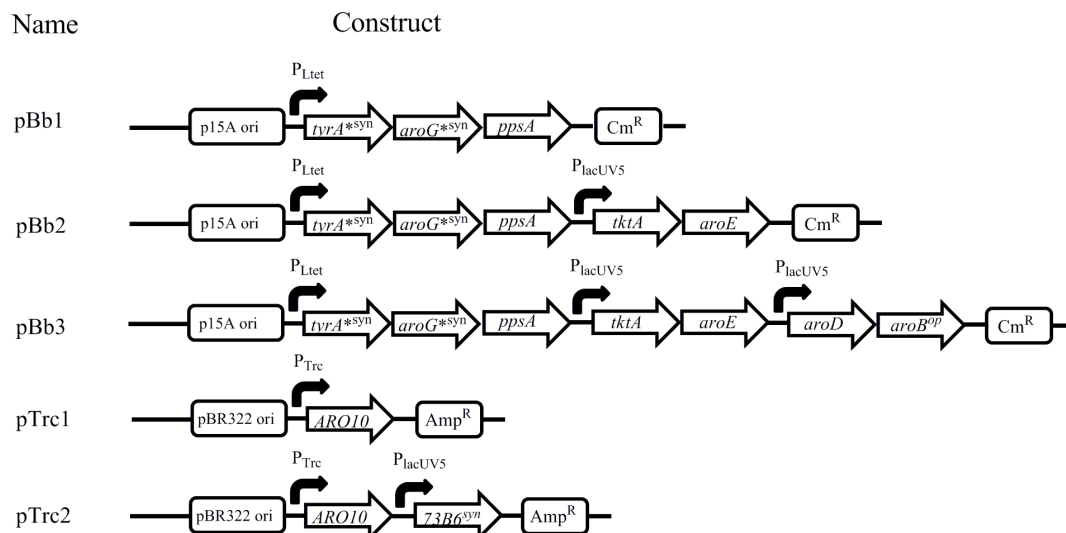


**Figure 2 | Plasmids construction.** Plasmids pBb1, pBb2 and pBb3 containing L-tyrosine pathway genes were used to stepwise enhance metabolic flux toward 4-hydroxyphenylpyruvate (2); plasmids pTrc1 and pTrc2 harbored genes encoding for enzymes involved in biosynthesis of tyrosol and salidroside.

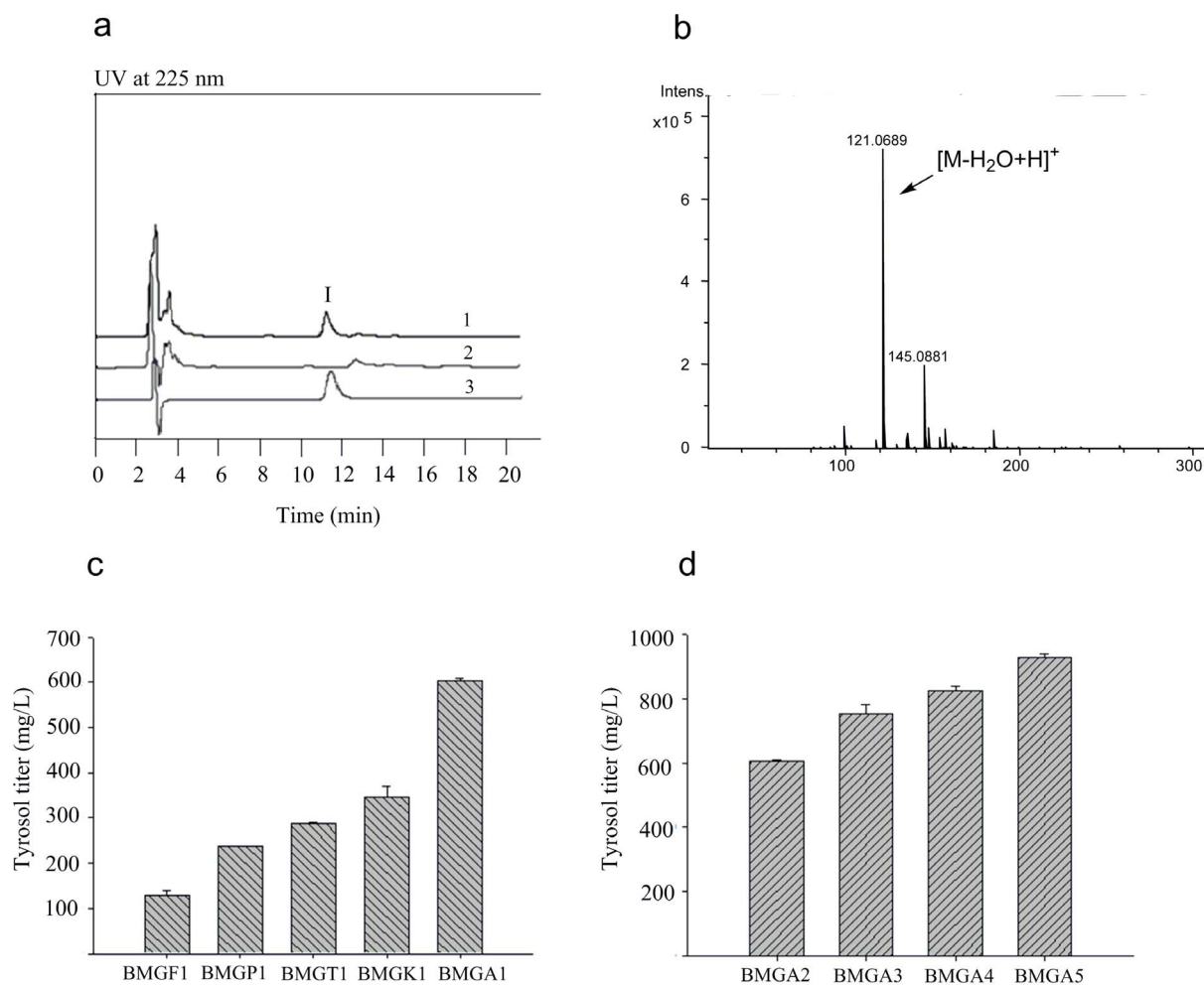


**Figure 3 | Production of tyrosol (3) in recombinant strains.** (a) HPLC analysis of tyrosol (3) production in the fermentation supernatant of recombinant strains. 1. BMGF1, *E. coli* MG1655 ( $\Delta feaB$ ) harboring plasmid pTrc1 ( $P_{Trc}$ -ARO10); 2. BMGF0, *E. coli* MG1655 ( $\Delta feaB$ ) harboring empty vector pTrcHisB (control); 3. Standard tyrosol (3). (b) Mass spectrum of tyrosol (3) from fermentation supernatant of strain BMGF1. (c) The influence of gene deletions on the tyrosol production. All the strains derived from BMGF1. The genes *pykA*, *tyrR*, *pykF* and *pheA* were sequentially deleted to enhance the metabolic flux toward 4-hydroxyphenylpyruvate (2), resulting strains BMGP1, BMGT1, BMGK1 and BMGA1. (d) The influence of genes overexpression on the tyrosol production. BMGA2, BMGA3, BMGA4 and BMGA5 were derived from BMGA1 harboring empty vector pBb0 (as control), pBb1 ( $P_{LtetO-1}$ -*tyrA*<sup>\*syn</sup>-*aroG*<sup>\*syn</sup>-*ppsA*), pBb2 ( $P_{LtetO-1}$ -*tyrA*<sup>\*syn</sup>-*aroG*<sup>\*syn</sup>-*ppsA* and  $P_{lacUV5}$ -*tktA*-*aroE*) and pBb3 ( $P_{LtetO-1}$ -*tyrA*<sup>\*syn</sup>-*aroG*<sup>\*syn</sup>-*ppsA*,  $P_{lacUV5}$ -*tktA*-*aroE* and  $P_{lacUV5}$ -*aroD*-*aroB*<sup>op</sup>), respectively. Three replicates were performed, and the error bars represented standard deviation.

and *TyrA*<sup>\*</sup> enzymes, are usually used to overcome the inhibition of the end product to enhance the accumulation of *L*-tyrosine<sup>32</sup>. Secondly, we expressed the *ppsA* and *tktA* genes, aiming to increase the supply of the two precursors involved in the aromatic amino acid biosynthesis, PEP and erythrose-4-phosphate (E4P). This step was based on the early reports that overexpression of *ppsA* and *tktA* genes encoding phosphoenolpyruvate synthase and transketolase, respectively, increases the yield of DAHP, approaching the theoretical limit yield<sup>33,34</sup>. Thirdly, *aroE*, *aroD* and *aroB*<sup>op</sup>, encoding shikimate dehydrogenase, 3-dehydroquinate (DHQ) dehydratase, and DHQ synthase, respectively, were overexpressed to further tune up the biosynthesis of compound 2. *AroE*, instead of its isozyme *YdiB*, was used owing to its binding specificity to shikimate, a crucial metabolite in the common pathway of aromatic amino acids; in contrast, *YdiB* was reported to favor formation of the by-product, quinate<sup>35</sup>. In a previous study, Juminaga et al. reported a relatively low level of *AroB* protein in *E. coli*, and analysis of the *aroB* nucleotide sequence revealed several rare codons at the beginning of the gene sequence<sup>36</sup>. To improve *aroB* expression, the first 15 codons were optimized by removing rare codons<sup>36</sup> designated as *aroB*<sup>op</sup>, thereby improving the production

of *AroB* proteins. We assembled the genes of *L*-tyrosine from the aforementioned pathway into three operons as gene clusters:  $P_{LtetO-1}$ -*tyrA*<sup>\*syn</sup>-*aroG*<sup>\*syn</sup>-*ppsA* (operon 1),  $P_{lacUV5}$ -*tktA*-*aroE* (operon 2), and  $P_{lacUV5}$ -*aroD*-*aroB*<sup>op</sup> (operon 3). These genes were sequentially cloned into the vector pBb0, a derivative of pBbA5c, to yield the plasmids pBb1 with operon 1, pBb2 with operons 1 and 2, and pBb3 with all 3 operons. These plasmids were individually transferred into the *E. coli* strain BMGA, harboring the plasmid pTrc1, thus generating strains BMGA3, BMGA4, and BMGA5. The yield of tyrosol (3) in these strains was found to be elevated to 752.6 mg/L, 824.9 mg/L, and 926.9 mg/L, progressively (Fig. 3d).

**Glucosylation of tyrosol in the recombinant *E. coli* strain.** UGT73B6 isolated from the plant *R. sachalinensis* was reported to display the glucosylation activity, thereby converting tyrosol (3) to salidroside (1). UGT73B6 was codon-optimized to make it suitable for its expression in *E. coli*. It was then introduced into the tyrosol (3) overproducing strain, BMGA5, to evaluate the production of salidroside. The resulting strain was designated as BMGA6.

The supernatant of the BMGA6 fermentation broth was first analyzed by HPLC and HR-ESI-MS, and further compared with the





standard salidroside (1). As shown in Fig. 4a, the strain BMGA6 carrying 73B6<sup>syn</sup> produced two new compounds besides tyrosol (3), which corresponded to the peaks II and III in the HPLC chromatogram. Compound II showed a retention time,  $t_R$ , of 8.8 min (Fig. 4a; peak II) and the molecular ion  $[M + NH_4]^+$  at  $m/z = 318.2950$  (Fig. 4b), which synchronized with the standard salidroside (1). The structure was further confirmed by  $^1H$  NMR spectroscopic analysis (Fig. S1) and compared to that of standard salidroside (1)<sup>37</sup>. The other compound (Fig. 4a; peak III,  $t_R$  5.4 min) showed a molecular ion at  $m/z$  318.1534 ( $[M + NH_4]^+$ ), as determined by HR-ESI-MS (Fig. 4d). We suspected the compound corresponding to peak III to be a derivative of tyrosol with glucosylation at the phenolic position (Fig. 4c). This compound was further purified from the extracts of the 1 L fermentation broth by semi-preparative HPLC, and analyzed by 1D and 2D-NMR spectroscopy. On the basis of  $^1H$ ,  $^{13}C$ , COSY, HSQC, and HMBC spectroscopic analyses, the structure of compound III was unambiguously determined as icariside D2 (4), with the glucoside added to the hydroxyl group on the benzene ring of tyrosol (3), rather than on the side chain of tyrosol (3), as displayed by salidroside (1) (Table 2; Fig. 4c). Icariside D2 (4) is a homolog of gastrodin (7) (Fig. 4c), with an extra methylene bridge (-CH<sub>2</sub>- unit) in the side chain. The phenolic glucoside, gastrodin (7), is a main active constituent of the widely known Chinese medicine, *Tianma* (*Gastrodia elata*) Blume, and has been used to treat various ailments,

such as headache, dizziness, vertigo, and convulsive illnesses, as part of the traditional medicine<sup>38</sup>. As a homologue of gastrodin (7), investigation on the potential pharmaceutical value of icariside D2 (4) may prove beneficial. The productions of salidroside (1), icariside D2 (4) and tyrosol were further measured in the fermentation broth of BMGA6, with titers of 56.9 mg/L, 63.2 mg/L and 764.6 mg/L, respectively.

## Discussion

To the best of our knowledge, this is the first report on the development of a unique artificial biosynthetic pathway in *E. coli* for the production of salidroside (1) from glucose. The protocol was successfully carried out using yeast pyruvate decarboxylase ARO10, endogenous ADHs, and glycosyltransferase UGT73B6 from *Rhodiola*. In order to streamline metabolic flux towards the production of aglycon tyrosol (3) from glucose, metabolic engineering of the L-tyrosine biosynthesis pathway (including gene deletion and over-expression) was performed. The regulatory gene, *tyrR*, and several genes involved in other competing pathways, *pykA*, *pykF*, and *pheA*, were deleted from the *E. coli* chromosome. A combined expression of *tyrA* (*tyrA*<sup>\*syn</sup>), *aroG* (*aroG*<sup>\*syn</sup>), *ppsA*, *tktA*, *aroE*, *aroD*, and *aroB*<sup>pp</sup>, coding for various enzymes of the L-tyrosine pathway, was found to be efficient in elevating the production of tyrosol (3). Finally, a maximum yield of 56.9 mg/L was obtained for salidroside (1). The

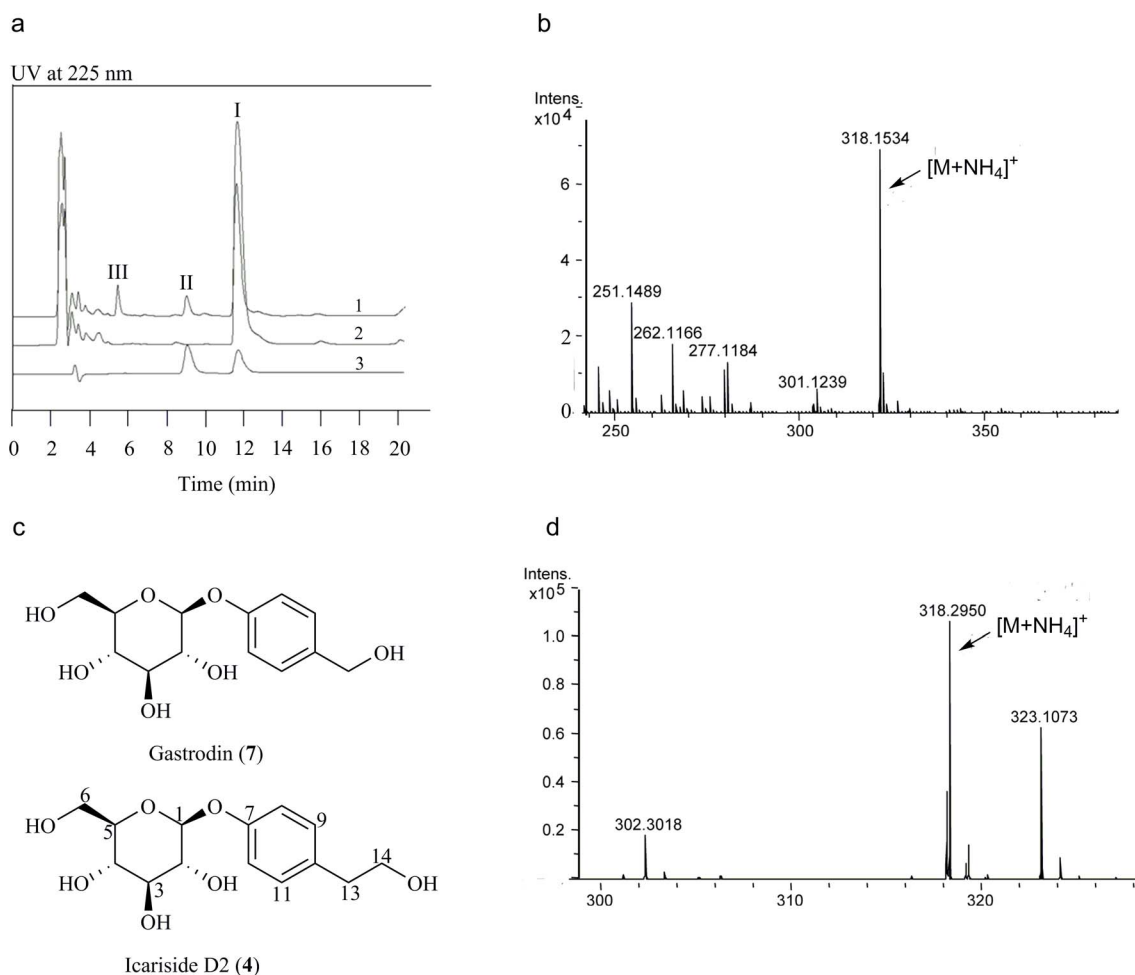


**Figure 4** | Salidroside (1) and icariside D2 (4) were produced by metabolically engineered strain carrying *Rhodiola*-derived glycosyltransferase. (a) HPLC analysis of tyrosol (3) and glycosylated derivatives in fermented supernatant sample of strains. 1. BMGA6 derived from BMGA5 by introduction of glycosyltransferase UGT73B6; 2. BMGA5 was a tyrosol over-producing strain; 3. Tyrosol (3) and salidroside (1) standard. (b) HR-ESI-MS of salidroside (3) from fermented supernatant of BMGA6. (c) Gastrodin (7), a main bioactive component from *Tianma* and its homolog icariside D2 (4). (d) HR-ESI-MS of icariside D2 (4) from fermented supernatant of strain BMGA6.

Table 2 | <sup>1</sup>H and <sup>13</sup>C NMR, HMBC, <sup>1</sup>H-<sup>1</sup>H COSY data for compound icariside D2 (4) (DMSO-*d*<sub>6</sub>, 600, 150 MHz, TMS, δ ppm)

position	δ <sub>C</sub>	δ <sub>H</sub> (J in Hz)	<sup>1</sup> H- <sup>1</sup> H COSY	HMBC
1	101.1, CH	4.78 d (6.0)	2	3, 7
2	73.7, CH	3.23 m		1, 3
3	77.1, CH	3.25 m	4	2
4	70.2, CH	3.15 m		3
5	77.5, CH	3.30 m	4	1, 4, 6
6	61.2, CH <sub>2</sub>	3.45 m, 3.68 m	5	4
7	156.2, C			
8	116.5, CH	6.92 d (12.0)	9	7, 10
9	130.1, CH	7.11 d (12.0)		7, 13
10	133.2, C			
11	130.1, CH	7.11 d (12.0)	12	7, 10
12	116.5, CH	6.92 d (12.0)		
13	56.2, CH <sub>2</sub>	2.65 t (6.0)	14	10, 11, 14
14	62.9, CH <sub>2</sub>	3.55 m		10
2-OH		5.25 d (6.0)	5	2, 3
3-OH		5.05 d (6.0)	3	
4-OH		4.99 d (6.0)	4	
6-OH		4.53 t (6.0)	6	5, 6
14-OH		4.59 t (6.0)	14	

present research may lead to the development of a simple and economical process for the large-scale microbial production of salidroside (1). In the future, the supply of UDP-glucose needs to be enhanced via metabolic engineering for the production of high levels of salidroside. Improvement in the enzymatic activities of the glucosyltransferase, UGT73B6, by protein engineering is also currently being undertaken in our lab.

It was interesting to discover the enzymatic activity of UGT73B6 attaching glucose to the phenol position of tyrosol (3), which was not observed in any previous study<sup>29</sup>. Nevertheless, the functional diversity and promiscuity of plant-specific UGTs are common, and many UGTs are known to exhibit broad substrate specificity<sup>39</sup>. Glycosyltransferases are important tools to generate novel glycosylated derivatives<sup>40,41</sup>. We identified UGT73B6 as a glucosyltransferase through *in vivo* experiments; in the process, we have revealed a flexible UGT, which might present a novel tool to produce natural glycosylated products with improved biological activities.

## Methods

**Bacterial strains and plasmids.** The bacterial strains and plasmids used in this study are listed in Table 1. All gene-deletion strains were derived from *E. coli* MG1655 by using the classical λ Red homologous recombination method<sup>42</sup>. The primers used for the amplification of DNA fragments for targeted genes are listed in Table S1.

**Pathway and plasmid construction.** The artificially constructed pathway of salidroside (1) production in *E. coli* is shown in Fig. 1. All the PCR primers are listed in Table S2. The constructed plasmids were confirmed by enzyme digestion and DNA sequencing. A list of plasmids and strains used in this study are presented in Table 1.

The codon-optimized variant of the *UGT73B6* gene (GenBank, AY547304) and two mutant genes encoding AroG\* (\*feed-back inhibition resistance) (Asp146 to Asn)<sup>43</sup> and TyrA\* (Met53 to Ile and Ala354 to Val)<sup>44</sup>, were synthesized by Shanghai Genaray Biotech Co. Ltd., and denoted as 73B6<sup>syn</sup>, *aroG*\*<sup>syn</sup>, and *tyrA*\*<sup>syn</sup>, respectively. The corresponding amino acids for the synthesized genes are provided in Supplementary Table S3. The pyruvate decarboxylase gene, *ARO10* (GenBank, NC\_001136), was amplified from *Saccharomyces cerevisiae* S288 genome, while the genes *ppsA*, *aroE*, *aroD*, and *aroB* were amplified from the genome of *E. coli* MG1655. To improve the expression of *AroB*, rare codons found within the first 15 codons of *AroB* were optimized<sup>35</sup> and designated as *aroB*<sup>op</sup>. All the genes were designed and amplified with their own ribosome binding sites.

Two plasmid systems were used to construct the biosynthetic pathways of tyrosol (3) and salidroside (1). pTrcHisB was used as a vector for constructing pTrc series plasmids, which contained the genes, *ARO10* and *UGT73B6* (Fig. 2). *ARO10* was cloned into pTrcHisB, generating the plasmid pTrc1. The 73B6<sup>syn</sup> gene was initially cloned into pTrcHisB, and PCR was carried out with the resulting plasmid to amplify the gene fragment, 73B6<sup>syn</sup>, under the control of a *trc* promoter. Subsequently, the PCR product was digested and cloned into pTrc1 to generate plasmid pTrc2, carrying *ARO10* and 73B6<sup>syn</sup>.

pBbA5c<sup>45</sup> was used as the starting plasmid to construct the gene clusters of L-tyrosine pathway and was further modified with new multi-cloning sites, thereby

yielding pBb0. *tyrA*\*<sup>syn</sup>, *aroG*\*<sup>syn</sup>, and *ppsA* were amplified via PCR and sequentially cloned into pBb0, in an operon driven by the P<sub>Ltet</sub> promoter, thus generating plasmid pBb1. The genes *tktA*, and *aroE* were sequentially cloned into pBb0, and PCR was conducted with the resulting plasmid harboring *tktA* and *aroE* as the template, to amplify the fragment containing the gene cluster. The DNA fragment was cloned into pBb1 as a second operon under the control of a P<sub>lacUV5</sub> promoter, yielding plasmid pBb2. Similarly, *aroD* and *aroB*<sup>op</sup> genes were incorporated into pBb2 driven by a P<sub>lacUV5</sub> promoter, generating plasmid pBb3 (Table 1; Fig. 2). The detailed protocols for cloning and plasmid construction are described in the Supplementary Material.

**Culturing of the recombinant *E. coli* strains.** All strains were cultivated in modified M9 medium (M9Y) containing 1 × M9 minimal salts, 5 mM MgSO<sub>4</sub>, 0.1 mM CaCl<sub>2</sub>, 2% (w/v) glucose, supplemented with 0.025% (w/v) yeast extract. Appropriate amounts of antibiotics (25 μg/mL chloramphenicol, 50 μg/mL ampicillin, and 100 μg/mL streptomycin) were supplemented to the medium, when needed. Isopropyl β-D-thiogalactopyranoside (IPTG) was added into the medium at a final concentration of 0.1 mM.

Single colonies of the engineered *E. coli* strains harboring the recombinant plasmids were inoculated in 5 mL liquid LB medium containing appropriate antibiotics, and allowed to grow overnight at 37°C. The culture was then diluted 1:100 with 50 mL fresh LB medium and incubated in a gyratory shaker incubator at 37°C, 200 rpm. When the absorbance of the culture (measured at 600 nm) reached to about 0.6–0.8, IPTG was added at 25°C for 24 h to induce recombinant protein expression. Subsequently, the cells were recovered by centrifugation, washed once, resuspended in 50 mL M9Y medium, and cultured at 30°C for 48 h for the extraction of compounds and further analysis. The shake-flask experiments were conducted in triplicates.

**Analysis of secondary metabolites from the recombinant *E. coli* strains.** For the analysis of tyrosol (3), 10 μL supernatant from the fermented broth was analyzed by High-performance liquid chromatography (HPLC) while for the analysis of salidroside (1) and icariside D2 (4), 50 μL of the supernatant was evaluated through HPLC. Standard tyrosol and salidroside (Aladdin chemistry Co. Ltd) were used as reference for the analysis. HPLC analysis was performed on an SHIMADZU system with UV detector. The products were detected at 225 nm under room temperature. The conditions used were as follows: solvent A = 0.1% methanoic acid in H<sub>2</sub>O; solvent B = methanol; flow rate = 1 mL min<sup>-1</sup>; 0–20 min 80% A and 20% B; 21–45 min 80% A and 20% B to 100% B (linear gradient); 46–50 min 100% B. The column used was Agela Innoval C18, 4.6 × 250 mm with a particle size of 5 μm. For the quantification of tyrosol (3), salidroside (1), and icariside D2 (4) in culture media, standard calibration curves were generated with a series of known concentrations of the standard dissolved in culture media. The R<sup>2</sup> coefficient for the calibration curves was higher than 0.999. Samples were diluted as required, in order to fall into the concentration range of the calibration curves.

**HPLC-MS analysis.** HPLC-MS was performed on an Agilent 1260 system with 1260 Infinity UV detector and a Bruker microQ-TOF II mass spectrometer equipped with an ESI ionization probe. For the analysis of tyrosol and its derivatives, the HPLC conditions used were as follows: solvent A = 0.144% ammonium acetate in H<sub>2</sub>O; solvent B = methanol; flow rate = 1 mL min<sup>-1</sup>; 0–5 min 95% A and 5% B, 6–45 min 95% A and 5% B to 100% B (linear gradient), and 46–55 min 100% B. The column



used was Agela Innoval C18, 4.6 × 250 mm with a particle size of 5 μm. The products were detected at 225 nm.

**Isolation of salidroside (1) and icaricide D2 (4).** To extract salidroside (1) and icaricide D2 (4) from the broth, 1 L of the fermentation broth was centrifuged after cultivation, and the supernatant was incubated with resin (HP-20) for 2 h. The resin was subsequently collected by centrifugation, washed once with distilled water and then washed with 50 mL methanol. Further, the methanol layer was collected by centrifugation and concentrated under reduced pressure. The residue was then dissolved in 2 mL methanol, and was purified by semi-preparative HPLC performed on a Shimadzu LC-6 AD with SPD-20A detector (solvent A = 0.1% methanoic acid in H<sub>2</sub>O; solvent B = methanol; solvent A/B = 3:1; flow rate = 8 mL min<sup>-1</sup>). A Shim-pack PREP-ODS (H) kit (20 × 250 mm; particle size, 5 μm) was used.

**NMR analysis.** NMR spectra were recorded on a Bruker AVANCE III 600 spectrometer using TMS as the internal standard, and chemical shifts were recorded as δ values. Details of the NMR data are presented in Table 2.

- Ma, L. Q. *et al.* Molecular cloning and overexpression of anovel UDP glucosyltransferase elevating salidroside levels in *Rhodiola sachalinensis*. *Plant Cell Rep* **26**, 989–999 (2007).
- Xu, J. F., Su, Z. G. & Feng, P. S. Activity of tyrosol glucosyltransferase and improved salidroside production through biotransformation of tyrosol in *Rhodiola sachalinensis* cell cultures. *J Biotechnol* **61**, 69–73 (1998).
- Qu, Z. Q., Zhou, Y. & Zeng, Y. S. Protective effects of a *Rhodiola Crenulata* extract and salidroside on hippocampal neurogenesis against Streptozotocin-induced neural injury in the rat. *PLoS ONE* **7**(1), e29641 (2012).
- Yang, Y. N. *et al.* Lignans from the root of *Rhodiola crenulata*. *J Agric Food Chem* **60**, 964–972 (2012).
- Mao, G. X. *et al.* Protective role of salidroside against aging in a mouse model induced by D-galactose. *Biomed Environ Sci* **23**, 161–166 (2010).
- Ouyang, J. F. *et al.* In-vitro promoted differentiation of mesenchymal stem cells towards hepatocytes induced by salidroside. *J Pharm Pharmacol* **62**, 530–538 (2010).
- Bonanome, A. *et al.* Evidence of postprandial absorption of olive oil phenols in humans. *Nutr Metab Cardiovasc Dis* **10**, 111–120 (2000).
- Udintsev, S. N. & Schachkov, V. P. Decrease of cyclophosphamide haematotoxicity by *Rhodiola rosea* root extract in mice with Ehrlich and Lewis transplantable tumors. *Eur J Cancer* **27**, 1182 (1991).
- Gupta, V. *et al.* A dose dependent adaptogenic and safety evaluation of *Rhodiola imbricata* Edgew. a high altitude rhizome. *Food Chem Toxicol* **46**, 1645–1652 (2008).
- Di Benedetto, R. *et al.* Tyrosol, the major extra virgin olive oil compound, restored intracellular antioxidant defenses in spite of its weak antioxidative effectiveness. *Nutr Metab Cardiovasc Dis* **17**, 535–545 (2007).
- Dudley, J. I. *et al.* Does white wine qualify for French paradox? Comparison of the cardioprotective effects of red and white wines and their constituents: resveratrol, tyrosol, and hydroxytyrosol. *J Agric Food Chem* **56**, 9362–9373 (2008).
- Puel, C. *et al.* Major phenolic compounds in olive oil modulate bone loss in an ovariectomy/inflammation experimental model. *J Agric Food Chem* **56**, 9417–9422 (2008).
- Liu, S. H., Pan, I. H. & Chu, I. M. Inhibitory effect of phydroxybenzyl alcohol on tyrosinase activity and melanogenesis. *Biol Pharm Bull* **30**, 1135–1139 (2007).
- Giovannini, L. *et al.* Inhibitory activity of the white wine compounds, tyrosol and caffeic acid, on lipopolysaccharide induced tumor necrosis factor-α release in human peripheral blood mononuclear cells. *Int J Tissue React* **24**, 53–56 (2002).
- Lan, X. *et al.* Engineering salidroside biosynthetic pathway in hairy root cultures of *Rhodiola crenulata* based on metabolic characterization of tyrosine decarboxylase. *PLoS ONE* **8**(10), e75459 (2013).
- Wu, S. X., Zu, Y. G. & Wu, M. High yield production of salidroside in the suspension culture of *Rhodiola sachalinensis*. *J Biotechnol* **106**, 33–43 (2003).
- Zhang, S. Q. *et al.* A new approach to synthesis of salidroside (Chinese). *Chin J Med Chem* **7**, 256–258 (1997).
- Boghigian, B. A., Zhang, H. & Pfeifer, B. A. Multi-factorial engineering of heterologous polyketide production in *Escherichia coli* reveals complex pathway interactions. *Biotechnol Bioeng* **108**, 1360–1371 (2011).
- Marienhagen, J. & Bott, M. Metabolic engineering of microorganisms for the synthesis of plant natural products. *J Biotechnol* **163**, 166–78 (2013).
- Lin, Y. H. *et al.* Combinatorial biosynthesis of plant-specific coumarins in bacteria. *Metab Eng* **18**, 69–77 (2013).
- Lin, Y. H., Rachit, J. & Yan, Y. J. Microbial production of antioxidant food ingredients via metabolic engineering. *Curr Opin Biotech* **26**, 71–78 (2014).
- Huang, Q., Lin, Y. H. & Yan, Y. J. Caffeic acid production enhancement by engineering a phenylalanine over-producing *Escherichia coli* strain. *Biotechnol Bioeng* **110**, 3188–96 (2013).
- Lin, Y. H. *et al.* Microbial biosynthesis of the anticoagulant precursor 4-hydroxycoumarin. *Nat Commun* **4**, 2603 (2013).
- Lin, Y. H. *et al.* Extending shikimate pathway for the production of muconic acid and its precursor salicylic acid in *Escherichia coli*. *Metab Eng* **23**, 62–9 (2014).

- Lin, Y. H. *et al.* Engineering bacterial phenylalanine 4-hydroxylase for microbial synthesis of human neurotransmitter precursor 5-hydroxytryptophan. *ACS Synth Biol* **3**, 497–505 (2014).
- Satoh, Y. *et al.* Engineering of a tyrosol-producing pathway, utilizing simple sugar and the central metabolic tyrosine, in *Escherichia coli*. *J Agric Food Chem* **60**, 979–984 (2012).
- Hazelwood, L. A. *et al.* The Ehrlich pathway for fusel alcohol production: a century of research on *Saccharomyces cerevisiae* metabolism. *Appl Environ Microbiol* **74**, 2259–66 (2008).
- Sentheshanmuganathan, S. & Elsdén, S. R. The mechanism of the formation of tyrosol by *Saccharomyces cerevisiae*. *Biochem J* **69**, 210–218 (1958).
- Yu, H. S. *et al.* Characterization of glycosyltransferases responsible for salidroside biosynthesis in *Rhodiola sachalinensis*. *Phytochemistry* **72**, 862–870 (2011).
- Bongaerts, J. *et al.* Metabolic engineering for microbial production of aromatic amino acids and derived compounds. *Metab Eng* **3**, 289–300 (2001).
- Polen, T. *et al.* The global gene expression response of *Escherichia coli* to L-phenylalanine. *J Biotechnol* **115**, 221–237 (2005).
- Chavez-Bejar, M. I. *et al.* Metabolic engineering of *Escherichia coli* for L-tyrosine production by expression of genes coding for the chorismate mutase domain of the native chorismate mutase-prephenate dehydratase and a cyclohexadienyl dehydrogenase from *Zymomonas mobilis*. *Appl Environ Microbiol* **74**, 3284–3290 (2008).
- Patnaik, R. & Liao, J. C. Engineering of *Escherichia coli* central metabolism for aromatic metabolite production with near theoretical yield. *Appl Environ Microbiol* **60**, 3903–3908 (1994).
- Patnaik, R., Spitzer, R. G. & Liao, J. C. Pathway engineering for production of aromatics in *Escherichia coli*: confirmation of stoichiometric analysis by independent modulation of AroG, TktA, and Pps activities. *Biotechnol Bioeng* **46**, 361–370 (1995).
- Juminaga, D. *et al.* Modular engineering of L-tyrosine production in *Escherichia coli*. *Appl Environ Microbiol* **78**, 89–98 (2012).
- Humphreys, D. P. *et al.* High-level periplasmic expression in *Escherichia coli* using a eukaryotic signal peptide: importance of codon usage at the 5' end of the coding sequence. *Protein Expr Purif* **20**, 252–264 (2000).
- Yu, P. *et al.* X-ray crystal structure and antioxidant activity of salidroside, a phenylethanoid glycoside. *Chem Biodivers* **4**, 508–513 (2007).
- Ojemann, L. M. *et al.* Tian ma, an ancient Chinese herb, offers new options for the treatment of epilepsy and other conditions. *Epilepsy Behav* **8**, 376–383 (2006).
- Taguchi, G. *et al.* Molecular cloning and heterologous expression of novel glucosyltransferases from tobacco cultured cells that have broad substrate specificity and are induced by salicylic acid and auxin. *Eur J Biochem* **268**, 4086–4094 (2001).
- Erb, A. *et al.* A bacterial glycosyltransferase gene toolbox: generation and applications. *Phytochemistry* **70**, 1812–1821 (2009).
- Gantt, R. W., Peltier-Pain, P. & Thorson, J. S. Enzymatic methods for glycol (diversification/randomization) of drugs and small molecules. *Nat Prod Rep* **28**, 1811–1853 (2011).
- Datsenko, K. A. & Wanner, B. L. One-step inactivation of chromosomal genes in *Escherichia coli* K-12 using PCR products. *Proc Natl Acad Sci USA* **97**, 6640–6645 (2000).
- Kikuchi, Y., Tsujimoto, K. & Kurahashi, O. Mutational analysis of the feedback sites of phenylalanine-sensitive 3-deoxy-D-arabino-heptulosonate-7-phosphate synthase of *Escherichia coli*. *Appl Environ Microbiol* **63**, 761–762 (1997).
- Lutke-Eversloh, T. & Stephanopoulos, G. Feedback inhibition of chorismate mutase/prephenate dehydrogenase (TyrA) of *Escherichia coli*: generation and characterization of tyrosine-insensitive mutants. *Appl Environ Microbiol* **71**, 7224–7228 (2005).
- Redding-Johanson, A. M. *et al.* Targeted proteomics for metabolic pathway optimization: application to terpene production. *Metab Eng* **13**, 194–203 (2011).

## Acknowledgments

This work was supported by grants from the 973 Program of China (2012CB721100), the 863 Program of China (2012AA02A704), the Sciences and Technology Planning projects of Tianjin city (13ZCZDSY05100), the National Natural Science Foundation of China (31300040 and 21302214). Tao Liu was supported by the 100 Talents Program of the Chinese Academy of Sciences.

## Author contributions

H.B., Y.B., X.Z., T.L. and Y.M. designed the experiments; Y.B., H.B., Y.Z., C.L., T.C. and X.L. performed the experiments; Y.B., H.B., Y.Z., C.L. and T.L. analyzed the data; H.B., Y.B., Y.Z. and T.L. wrote the paper; all authors reviewed the manuscript.

## Additional information

Supplementary information accompanies this paper at <http://www.nature.com/scientificreports>



**Competing financial interests:** This work has been included in a patent application by the Tianjin Institute of Industrial Biotechnology.

**How to cite this article:** Bai, Y. *et al.* Production of salidroside in metabolically engineered *Escherichia coli*. *Sci. Rep.* 4, 6640; DOI:10.1038/srep06640 (2014).



This work is licensed under a Creative Commons Attribution-NonCommercial-ShareAlike 4.0 International License. The images or other third party material in this

article are included in the article's Creative Commons license, unless indicated otherwise in the credit line; if the material is not included under the Creative Commons license, users will need to obtain permission from the license holder in order to reproduce the material. To view a copy of this license, visit <http://creativecommons.org/licenses/by-nc-sa/4.0/>